

# Dispersive reservoir influence on the superconducting phase qubit

A. H. Homid<sup>1,\*</sup>, A.-B. A. Mohamed<sup>2,3</sup> and H. A. Hessian<sup>3</sup>

<sup>1</sup> Faculty of Science, Al-Azhar University, Assiut, Egypt

<sup>2</sup> AL-Aflaj Community College, Salman Bin Abdulaziz University, Saudi Arabia

<sup>3</sup> Faculty of Science, Assiut University, Assiut, Egypt

## Abstract

In this article, an analytical description is presented based on the master equation. This master equation is formed from the system of superconducting phase qubit which is coupled to a torsional resonator and damped by a dispersive reservoir. An analytical approach for searching of some physical phenomena on the qubit system is presented, such as qubit inversion, purity and negativity. In addition, these phenomena are discussed for the resonance and off-resonance cases for many different initial states. From computational results, it is found that the mentioned phenomena depend on the dispersive reservoir parameter which leads to their death. However, the complete destruction of system coherence in the presence of dispersive reservoir leads to the death of entanglement between the qubit and torsional resonator.

**keywords:** Superconducting Phase Qubit; Density Matrix; Entanglement; Dispersive Reservoir.

## 1 Introduction

In the recent years, the quantum entanglement and mixedness are two biggest challenges of quantum information theory. Quantum entanglement is a very important quantum characteristic that has no classical counterpart. Also, quantum entanglement is necessary for the realization of quantum communication and the most important computational tasks, such as quantum teleportation [1], superdense coding [2] and so on. In addition, it is crucial to understand the fundamental aspects of quantum mechanics, including quantum measurement and quantum decoherence [3]. Consequently, no system can be completely isolated from its environment. Thus in real experimental situations due to the coupling environment, the entangled state inevitably loses its purity and becomes mixed.

Decoherence phenomenon is the most dangerous obstacle for all entanglement manipulations. However, the recent studies of decoherence effect for different systems are increased due to the variety of applications in areas as quantum optics and quantum information [4–7]. In fact, the interactions between a quantum system with the environment are caused two types of irreversible effects, e.g., quantum dissipation and quantum decoherence [8, 9]. The former will cause energy dissipation, and the latter will make the system degenerate from coherent

---

\*E-mail :ahomid86@gmail.com

state to classical state. Entanglement evolution under decoherence has attracted much interest and many researchers have studied it extensively based on various models in the view of environment-induced decoherence [10, 11].

In the previous years, some researchers have found that state entanglement can be decreased to zero abruptly and remained zero for a finite time. This phenomenon is called entanglement sudden death [12–16], where entanglement of two-qubit decays to zero in a finite time under the influence of pure vacuum noise [17]. Precisely, entanglement sudden death has been experimentally observed in an implementation using twin photons [18] and atomic ensembles [19]. In many efforts have been devoted to study various types of superconducting (SC) qubit which is considered as good candidate to solve this problem.

Nowadays, superconductors are viable elements and feasible within current experimental technology. SC qubit is represented a unique and its interesting approach to quantum information and quantum computation because it naturally allow strong coupling. Some aspects which are discussed through these systems: entanglement between a flux qubit and a superconducting quantum interference device (SQUID) [20] have been realized experimentally. In addition, there are other aspects: the strong coupling of a single photon to a SC qubit has been experimentally demonstrated [21] by using a one-dimensional transmission line resonator [22]. Recently, some quantum logic gates have proposed [23] by using a system consisting of a number of SC-charge qubits coupled to a resonator to study different quantum operations. Also, a new physical scheme for implementing a discrete quantum Fourier transform is proposed via SC qubits coupled to a single-mode SC-cavity [24]. However, the effect of environment cannot be neglected in these situations [25], because, the qubits are never isolated, but under some environmental influence.

Our purpose of this article is to give an analysis of the entanglement dynamics of a SC phase qubit coupled to a torsional resonator. Consequently, some phenomena, such as the qubit inversion, purity and negativity are theoretically investigated, mainly because such states are more physical and experimentally relevant. Thus we take into account decoherence and analyze its effect on these phenomena. Despite the complexity of the problem, the analytical descriptions of the exact solution of the master equation is presented.

This article is arranged as follows: The physical system of qubit with torsional resonator and its dynamics is provided in section 2. The influence of phase-damping on a SC qubit inversion and measures of entanglement is presented in section 3. Finally, the conclusions is demonstrated in section 4.

## 2 The physical system of qubit with torsional resonator and its dynamics

We introduce a theoretical description of the superconducting phase qubit coupled to a torsional resonator. A phase qubit with  $\kappa$  excess Cooper-pair charges consists of two superconducting islands connected to a superconducting electrode through two identical Josephson tunnel junctions of a small size with the same capacitance  $C_J$ , see Fig.1. If the phase qubit is working in a regime with  $k_B T \ll E_C \ll E_J$ , where  $E_J$ ,  $E_C$ ,  $k_B$  and  $T$  are Josephson energy, charging energy, Boltzmann constant and temperature, respectively. The Hamiltonian of the superconducting phase qubit can be described by the form [26]

$$\hat{H}_{qu} = \frac{(2e)^2}{2C_J} \kappa^2 - \frac{\hbar I_0}{2e} \left( \cos(\pi f_c) + \frac{I}{I_0} \Theta \right) \cos(\Theta - \pi f_c), \quad (1)$$

where  $\Theta$ ,  $I$ ,  $I_0$ , and  $f_c$  are the phase difference across the junction, bias current, junction critical current, and the external flux which is generated by a classical applied magnetic field, respec-

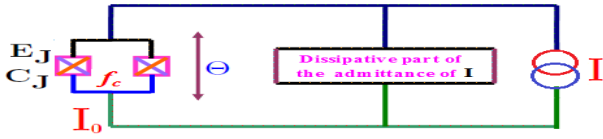


Figure 1: Circuit diagram of the phase qubit; a single Josephson junction with Josephson coupling energy  $E_J$  and Josephson capacitance  $C_J$  is driven with a bias current  $I$ . The rectangle in this diagram refer to dissipative part of the admittance of the bias current  $I$ .

tively. Moreover,  $\kappa$  and  $\Theta$  are quantum mechanical conjugate variables and satisfy  $[\kappa, \Theta] = -i$ .

In this study, the bias current  $I$  is assumed to be zero. The Josephson energy, and the charging energy for each junction also are assumed to be  $E_J = \hbar I_0/2e \sim 6.8 \times 10^{-21} J$  and  $E_C = \frac{(2e)^2}{2C_J} \sim 8.3 \times 10^{-27} J$  as estimated in [27]. Therefore, the effective Josephson coupling  $E_{J_e} = E_J \cos(\pi f_c)$  of phase qubit is controlled by the external flux  $f_c$ . If the phase different  $\Theta$  is confined to the period  $\pi f_c$ , the states of a single qubit are restricted to a two lowest-energy states  $|g\rangle$  and  $|e\rangle$ . Hence, the Hamiltonian (1) can be converted to a spin representation as follows:

$$\hat{H}_{qu} = -\frac{\hbar\omega_z}{2}\hat{\sigma}_z, \quad (2)$$

where  $\omega_z \sim \frac{\sqrt{2E_C E_{J_e}}}{\hbar}$  is the frequency of the phase qubit, and  $\hat{\sigma}_z$  is the usual Pauli spin operator.

The torsional resonator mode is described by a harmonic oscillator-like Hamiltonian as follows [28]

$$\hat{H}_{mode} = \frac{P_{\top}^2}{2I_m} + \frac{1}{2}I_m\omega_v^2\top^2, \quad (3)$$

where  $P_{\top}$  is the angular momentum conjugate to  $\top$  and  $\top \in [0, 2\pi]$ . The fluctuations of the angle  $\top$  can be described by the fluctuation  $\top_0 = \sqrt{\hbar/I_m\omega_v}$  in the ground state, where  $I_m$ , and  $\omega_v$  are the rotational moment of inertia of the torsional resonator, and vibration frequency, respectively.

If we put the SC qubit in the torsional resonator, the effective flux is  $f_c = f' \sin \top$ . Hence,  $\top$  is measured relative to the direction of  $f_c$ ,  $E_J$  is the largest energy scale and coupling between

the qubit and torsional vibrational mode can be a large quantity. Thus, we consider the qubit is coupled to resonator mode. Also, the external magnetic field is parallelly applied to the phase qubit plane. Then the external field in this case is given by:  $f_c = f'(\top - \top_e)$ , where  $\top_e$  is the angle at equilibrium measured from the direction of  $f_c$ . In this work,  $f'$  is the maximum value of magnetic flux when the field is perpendicular to the qubit plane. If  $\top_e$  is non-zero, the coupling strength is decreased by factor  $\sin \top_e$ , so consider the angle  $\top_e = 0$ . However, one concludes that the total Hamiltonian restricted to the two states is given by:

$$\hat{H}_t = \hbar\omega\hat{a}^\dagger\hat{a} - \frac{\hbar\omega_z}{2}\hat{\sigma}_z + G(\hat{a} + \hat{a}^\dagger)\hat{\sigma}_x, \quad (4)$$

where  $(\hat{a}^\dagger)\hat{a}$  and  $(\hat{\sigma}^\dagger)\hat{\sigma}$  are the (creation) annihilation operators for the vibrational mode and phase qubit, respectively,  $G = \pi f' \sqrt{\frac{E_J\omega_z}{2I_m\omega}}$  is the constant coupling energy between the phase qubit and the torsional resonator, and  $\omega = \sqrt{\omega_v^2 + 2\pi^2 f'^2 E_J/I_m}$  is the torsional oscillator frequency. Because of the negative sign of the second term, the above Hamiltonian (4) in the counter-rotating wave approximation can be written as follows:

$$\hat{H} = \hbar\omega\hat{a}^\dagger\hat{a} - \frac{\hbar\omega_z}{2}\hat{\sigma}_z + G(\hat{a}\hat{\sigma}_- + \hat{a}^\dagger\hat{\sigma}_+). \quad (5)$$

Under the previous hypothesis, the non-unitary time evolution of present interaction system with taking into account the dissipative effect is given through the density operator. The density operator is described by a master equation of the form:

$$\hbar\dot{\hat{\rho}} = i[\hat{\rho}, \hat{H}] + \frac{\hbar\gamma}{2}(\hat{\sigma}_z\hat{\rho}\hat{\sigma}_z - \hat{\rho}), \quad (6)$$

where  $\gamma$  is a positive parameter that represents a dispersive reservoir (or phase damping of the qubit system). It is one of the variables that does not interchange energy with the qubit system. Dispersive reservoir of the qubit may occur due to dephasing interactions that might arise. For instance, the dispersive reservoir may occur from the elastic collisions in a qubit vapor. The exact solution for Eq.6 in the case of a high- $Q$  torsional resonator ( $\gamma/G \ll 1$ ) is obtained by analytic method. The used analytic method is presented by the dressed-states representation [29–31]. This representation is consisting of the complete set of Hamiltonian eigenfunctions. Here, the states  $|g\rangle$  and  $|e\rangle$  are corresponding to the higher energy and the lower energy, respectively. In the invariant subspace spanned by  $|e, n+1\rangle$  and  $|g, n\rangle$ , the eigenvalues and eigenfunctions of the Hamiltonian (5) are given by:

$$\hat{H}|\Psi_n^\pm\rangle = E_n^\pm|\Psi_n^\pm\rangle, \quad \hat{H}|e, 0\rangle = -\frac{\hbar\omega_z}{2}|e, 0\rangle, \quad (7)$$

with the abbreviations  $E_n^\pm = \hbar\omega(n + \frac{1}{2}) \pm R_n$ ,  $|\Psi_n^\pm\rangle = \beta_n^\mp|g, n\rangle \pm \beta_n^\pm|e, n+1\rangle$ ,  $\beta_n^\pm = \frac{1}{\sqrt{2}}\sqrt{1 \mp \frac{\delta}{R_n}}$ ,  $R_n = G\sqrt{(n+1) + (\frac{\delta}{G})^2}$ , and  $\delta = \frac{\hbar(\omega_z - \omega)}{2}$  is the detuning parameter which represents the difference between transition energy of qubit and torsional energy.

To obtain the analytical solution for Eq.6, we suppose that the qubit is initially in the general superposition of the excited state and ground state while the torsional resonator is assumed to be initially in a coherent state, that is

$$\hat{\rho}(0) = \left(\cos\theta|e\rangle + e^{i\varphi}\sin\theta|g\rangle\right)\left(\cos\theta|e\rangle + e^{i\varphi}\sin\theta|g\rangle\right)^\dagger \otimes |\alpha\rangle\langle\alpha|. \quad (8)$$

Consequently, the time-dependent analytical solution for the density matrix with the initial previous state is given by:

$$\hat{\rho}(t) = \rho_{ee}^{00}|e, 0\rangle\langle e, 0| + \sum_{n,m=0}^{\infty} \left\{ \rho_{gg}^{n,m}(t)|g, n\rangle\langle g, m| + \rho_{ge}^{n,m+1}(t)|g, n\rangle\langle e, m+1| \right. \\ \left. + \rho_{eg}^{n+1,m}(t)|e, n+1\rangle\langle g, m| + \rho_{ee}^{n+1,m+1}(t)|e, n+1\rangle\langle e, m+1| \right\}, \quad (9)$$

where all elements of the density matrix (9) are also functions in  $\theta, \varphi, \delta$ . The elements of the previous density matrix are given by the following formulas:

$$\rho_{ee}^{n+1,m+1}(t) = \begin{cases} x_n x_m^* e^{-iA_{n,m}t} \{ 2\beta_n^+ \beta_n^- \beta_m^+ \beta_m^- \sin^2 \theta [\mathbb{E}_{n,m}^{+-} \cos(R_{n,m}^{+-}t) - \mathbb{K}_{n,m}^{++} \cos(R_{n,m}^{++}t)] \\ + \xi_{n,m} \cos^2 \theta [(\beta_n^{+2} \beta_m^{+2} e^{-iR_{n,m}^{+-}t} + \beta_n^{-2} \beta_m^{-2} e^{iR_{n,m}^{+-}t}) \mathbb{E}_{n,m}^{+-} \\ + (\beta_n^{+2} \beta_m^{-2} e^{-iR_{n,m}^{++}t} + \beta_n^{-2} \beta_m^{+2} e^{iR_{n,m}^{++}t}) \mathbb{K}_{n,m}^{++}] \\ + \frac{\tilde{\alpha} \beta_m^+ \beta_m^- \sin 2\theta}{2\sqrt{n+1}} [(\beta_n^{+2} e^{-iR_{n,m}^{+-}t} - \beta_n^{-2} e^{iR_{n,m}^{+-}t}) \mathbb{E}_{n,m}^{+-} + (\beta_n^{-2} e^{iR_{n,m}^{++}t} - \beta_n^{+2} e^{-iR_{n,m}^{++}t}) \mathbb{K}_{n,m}^{++}] \\ + \frac{\tilde{\alpha}^* \beta_n^+ \beta_n^- \sin 2\theta}{2\sqrt{m+1}} [(\beta_m^{+2} e^{-iR_{n,m}^{+-}t} - \beta_m^{-2} e^{iR_{n,m}^{+-}t}) \mathbb{E}_{n,m}^{+-} + (\beta_m^{-2} e^{-iR_{n,m}^{++}t} - \beta_m^{+2} e^{iR_{n,m}^{++}t}) \mathbb{K}_{n,m}^{++}] \}, \\ \forall n \neq m; \\ |x_n|^2 \{ \sin^2 \theta [\Pi^{+,-} - v^{+,-}] + \xi_{n,n} \cos^2 \theta [\varpi^{+,-} + v^{+,-}] + \Omega^{+,-} + \Gamma^{+,-} \}, \\ \forall n=m. \end{cases}$$

$$\rho_{gg}^{n,m}(t) = \begin{cases} x_n x_m^* e^{-iA_{n,m}t} \{ \sin^2 \theta [(\beta_n^{-2} \beta_m^{-2} e^{-iR_{n,m}^{+-}t} + \beta_n^{+2} \beta_m^{+2} e^{iR_{n,m}^{+-}t}) \mathbb{E}_{n,m}^{+-} \\ + (\beta_n^{+2} \beta_m^{-2} e^{iR_{n,m}^{++}t} + \beta_n^{-2} \beta_m^{+2} e^{-iR_{n,m}^{++}t}) \mathbb{K}_{n,m}^{++}] \\ + 2\beta_n^+ \beta_n^- \beta_m^+ \beta_m^- \xi_{n,m} \cos^2 \theta [\mathbb{E}_{n,m}^{+-} \cos(R_{n,m}^{+-}t) - \mathbb{K}_{n,m}^{++} \cos(R_{n,m}^{++}t)] \\ + \frac{\tilde{\alpha} \beta_n^+ \beta_n^- \sin 2\theta}{2\sqrt{n+1}} [(\beta_m^{+2} e^{-iR_{n,m}^{+-}t} - \beta_m^{-2} e^{iR_{n,m}^{+-}t}) \mathbb{E}_{n,m}^{+-} + (\beta_m^{+2} e^{-iR_{n,m}^{++}t} - \beta_m^{-2} e^{iR_{n,m}^{++}t}) \mathbb{K}_{n,m}^{++}] \\ + \frac{\tilde{\alpha}^* \beta_m^+ \beta_m^- \sin 2\theta}{2\sqrt{m+1}} [(\beta_n^{-2} e^{-iR_{n,m}^{+-}t} - \beta_n^{+2} e^{iR_{n,m}^{+-}t}) \mathbb{E}_{n,m}^{+-} + (\beta_n^{+2} e^{iR_{n,m}^{++}t} - \beta_n^{-2} e^{-iR_{n,m}^{++}t}) \mathbb{K}_{n,m}^{++}] \}, \\ \forall n \neq m; \\ |x_n|^2 \{ \sin^2 \theta [\varpi^{+,-} + v^{+,-}] + \xi_{n,n} \cos^2 \theta [\Pi^{+,-} - v^{+,-}] - \Omega^{+,-} - \Gamma^{+,-} \}, \\ \forall n=m. \end{cases}$$

$$\rho_{eg}^{n+1,m}(t) = \begin{cases} x_n x_m^* e^{-iA_{n,m}t} \{ \beta_n^+ \beta_n^- \sin^2 \theta [(\beta_m^{-2} e^{-iR_{n,m}^{+-}t} - \beta_m^{+2} e^{iR_{n,m}^{+-}t}) \mathbb{E}_{n,m}^{+-} + (\beta_m^{+2} e^{-iR_{n,m}^{++}t} - \beta_m^{-2} e^{iR_{n,m}^{++}t}) \mathbb{K}_{n,m}^{++}] \\ + \beta_m^+ \beta_m^- \xi_{n,m} \cos^2 \theta [(\beta_n^{+2} e^{-iR_{n,m}^{+-}t} - \beta_n^{-2} e^{iR_{n,m}^{+-}t}) \mathbb{E}_{n,m}^{+-} + (\beta_n^{-2} e^{iR_{n,m}^{++}t} - \beta_n^{+2} e^{-iR_{n,m}^{++}t}) \mathbb{K}_{n,m}^{++}] \\ + \frac{\tilde{\alpha} \sin 2\theta}{2\sqrt{n+1}} [(\beta_n^{+2} \beta_m^{-2} e^{-iR_{n,m}^{+-}t} + \beta_n^{-2} \beta_m^{+2} e^{iR_{n,m}^{+-}t}) \mathbb{E}_{n,m}^{+-} + (\beta_n^{+2} \beta_m^{+2} e^{-iR_{n,m}^{++}t} + \beta_n^{-2} \beta_m^{-2} e^{iR_{n,m}^{++}t}) \mathbb{K}_{n,m}^{++}] \\ + \frac{\tilde{\alpha}^* \sin 2\theta}{\sqrt{m+1}} \beta_n^+ \beta_n^- \beta_m^+ \beta_m^- [\mathbb{E}_{n,m}^{+-} \cos(R_{n,m}^{+-}t) - \mathbb{K}_{n,m}^{++} \cos(R_{n,m}^{++}t)] \}, \\ \forall n \neq m; \\ |x_n|^2 \{ \beta_n^+ \beta_n^- \sin^2 \theta [(\beta_n^{-2} - \beta_n^{+2}) e^{-\frac{\gamma b n t}{2}} \mathbb{E}_{n,n}^{+-} + (\beta_n^{+2} e^{-iR_{n,n}^{++}t} - \beta_n^{-2} e^{iR_{n,n}^{++}t}) \mathbb{K}_{n,n}^{++}] \\ + \beta_n^+ \beta_n^- \xi_{n,n} \cos^2 \theta [(\beta_n^{+2} - \beta_n^{-2}) e^{-\frac{\gamma b n t}{2}} \mathbb{E}_{n,n}^{+-} + (\beta_n^{-2} e^{iR_{n,n}^{++}t} - \beta_n^{+2} e^{-iR_{n,n}^{++}t}) \mathbb{K}_{n,n}^{++}] \\ + \frac{\beta_n^{+2} \beta_n^{-2} \sin 2\theta (\tilde{\alpha} + \tilde{\alpha}^*)}{\sqrt{n+1}} e^{-\frac{\gamma b n t}{2}} \mathbb{E}_{n,n}^{+-} \\ + \frac{\sin 2\theta}{\sqrt{n+1}} [\frac{\tilde{\alpha}}{2} (\beta_n^{+4} e^{-iR_{n,n}^{++}t} + \beta_n^{-4} e^{iR_{n,n}^{++}t}) - \tilde{\alpha}^* \beta_n^{+2} \beta_n^{-2} \cos(R_{n,n}^{++}t)] \mathbb{K}_{n,n}^{++} \}, \\ \forall n=m. \end{cases}$$

Where

$$\begin{aligned}
\rho_{ge}^{n,m+1} &= (\rho_{eg}^{n+1,m})^\dagger, \quad \rho_{ee}^{00} = e^{-|\alpha|^2} \cos^2 \theta, \quad \tilde{\alpha} = \alpha e^{-i\varphi}, \quad \xi_{n,m} = \frac{|\alpha|^2}{\sqrt{(n+1)(m+1)}}, \\
x_n &= e^{(-\frac{|\alpha|^2}{2})} \frac{\alpha^n}{\sqrt{n!}}, \quad R_{n,m}^{+-} = R_n - R_m, \quad R_{n,m}^{++} = R_n + R_m, \\
\Delta_{n,m}^{+-} &= \frac{1}{2} [1 - (\beta_n^{+2} \beta_m^{+2} + \beta_n^{-2} \beta_m^{-2} - \beta_n^{+2} \beta_m^{-2} - \beta_n^{-2} \beta_m^{+2})], \\
\Delta_{n,m}^{++} &= \frac{1}{2} [1 + (\beta_n^{+2} \beta_m^{+2} + \beta_n^{-2} \beta_m^{-2} - \beta_n^{+2} \beta_m^{-2} - \beta_n^{-2} \beta_m^{+2})], \\
\mathbb{E}_{n,m}^{+-} &= e^{-\gamma t \Delta_{n,m}^{+-}}, \quad \mathbb{K}_{n,m}^{++} = e^{-\gamma t \Delta_{n,m}^{++}}, \quad b_n = 4\beta_n^{+2} \beta_n^{-2}, \quad A_{n,m} = \hbar\omega(n-m), \\
\Gamma^{+,-} &= \frac{\beta_n^+ \beta_n^- \sin 2\theta}{2\sqrt{n+1}} [\beta_n^{-2} (\tilde{\alpha} e^{iR_{n,n}^{++}t} + \tilde{\alpha}^* e^{-iR_{n,n}^{++}t}) - \beta_n^{+2} (\tilde{\alpha} e^{-iR_{n,n}^{++}t} + \tilde{\alpha}^* e^{iR_{n,n}^{++}t})] \mathbb{K}_{n,n}^{++}, \\
\Omega^{+,-} &= \frac{\beta_n^+ \beta_n^- \sin 2\theta (\tilde{\alpha} + \tilde{\alpha}^*)}{2\sqrt{n+1}} (\beta_n^{+2} - \beta_n^{-2}) e^{-\frac{\gamma b_n t}{2}} \mathbb{E}_{n,n}^{+-}, \\
\Pi^{+,-} &= [(\beta_n^{+4} + \beta_n^{-4}) \sinh(\frac{\gamma b_n t}{2}) + 2\beta_n^{+2} \beta_n^{-2} \cosh(\frac{\gamma b_n t}{2})] \mathbb{E}_{n,n}^{+-}, \\
\varpi^{+,-} &= [(\beta_n^{+4} + \beta_n^{-4}) \cosh(\frac{\gamma b_n t}{2}) + 2\beta_n^{+2} \beta_n^{-2} \sinh(\frac{\gamma b_n t}{2})] \mathbb{E}_{n,n}^{+-} \quad \text{and} \\
v^{+,-} &= 2\beta_n^{+2} \beta_n^{-2} \cos(R_{n,n}^{++}t) \mathbb{K}_{n,n}^{++}.
\end{aligned}$$

To calculate the asymptotic behavior of the density matrix, we set  $Gt \rightarrow \infty$ , as follows:

$$\begin{aligned}
\hat{\rho}(Gt \rightarrow \infty) &= \rho_{ee}^{00} |e, 0\rangle \langle e, 0| + \frac{1}{2} \sum_{n=0}^{\infty} |x_n|^2 \left( \sin^2 \theta + \xi_{n,n} \cos^2 \theta \right) \\
&\quad \times \left( |e, n+1\rangle \langle e, n+1| + |g, n\rangle \langle g, n| \right),
\end{aligned}$$

which is a statistically mixed state.

### 3 The influence of dispersive reservoir on some physical phenomena

In the current section, we study the existence of some phenomena of the previous system. In an effort to present a numerical characterization, we have performed some calculations for the properties quantity for a particular set of parameters, some of which can be considered as realistic, while some other parameters look perhaps too optimistic.

#### 3.1 SC qubit inversion phenomenon

The qubit inversion is one of the important dynamic variables of the properties of quantum mechanics. It gives information about the behavior of the qubit during the interaction period. Therefore, by using the analytic solution of the master equation and keeping in mind that the state  $|g\rangle$  is the one with higher energy, we discuss the effect of dispersive reservoir on qubit inversion, which is given by:

$$W_{qu}(t) = \rho_{ee}^{00} + \sum_i \left( \rho_{ee}^{ii}(t) - \rho_{gg}^{ii}(t) \right). \quad (10)$$

It is generally accepted that the revivals of inversion appears as a consequence of quantum coherence which are built up during the interaction between the resonator and the qubit.

Numerical calculations which indicate the influence of dispersive reservoir  $\frac{\gamma}{G}$  on qubit inversion is exhibited in Fig.2a, Fig.2b and Fig.2c. The time evolution of  $W_{qu}$  is plotted as a function of the scaled time  $\frac{Gt}{\pi}$  and  $\frac{\gamma}{G}$ , in the resonance case, for a different values of  $\theta$  and  $\alpha$ . In the absence of detuning effect and  $\frac{\gamma}{G}$ , see Fig.2a and Fig.2b, one finds that  $W_{qu}$  fluctuates around zero, and the collapse and revival phenomena start to appear. It is seen from Fig.2a

and Fig.2b a short period of collapse after onset of the interaction followed immediately by a reasonable revival period. After this period of collapse, one can not see another collapse period because of existence of interference in the fluctuation, so in these cases of  $\theta$  the revival period is not apparent. The reason for this is due to the value of coherence parameter  $\alpha$ . If  $\alpha = 6$ , the revival and collapse phenomena are more pronounced than the other case for different values of  $\theta$ , say  $\frac{\pi}{2}$ . This result is observed in Fig.2c. Furthermore, for many different values of  $\theta$ , the revival and collapse phenomena are more pronounced. Also, it is observed from Fig.2 that the periodic oscillations of  $W_{qu}$  between 1 as a maximum value and  $-1$  as a minimum value around 0.

If the dispersive reservoir parameter is regarded  $\frac{\gamma}{G} \neq 0$ , the time evolution of  $W_{qu}$  is shown in Figs.2a, Fig.2b and Fig.2c. At a weak dispersive reservoir, the collapses and revivals phenomenon is still observed for a short time. The increase of collapses region slowly due to the influence of the damping. But with large values of dispersive reservoir, the amplitude of revivals is greatly decreased. With  $\frac{\gamma}{G} > 0.1$ , all revivals are completely washed out, and the system is collapsed completely. This means that the probability of existence for the qubit in the state  $|g\rangle$  and  $|e\rangle$  are equal.

To investigate the influence of detuning parameter  $\frac{\delta}{G}$  and  $\frac{\gamma}{G}$  parameter on the behavior of qubit inversion, we display in Fig.2d the behavior of inversion in off-resonance case with  $\theta = \frac{\pi}{3}$ ,  $\frac{\delta}{G} = 6$  and  $\alpha = 3$ . Firstly, for  $\frac{\gamma}{G} = 0$ , one can observe from Fig.2d, the revivals and collapses phenomena are more pronounced than the case of  $\frac{\delta}{G} = 0$ , and the curve of qubit inversion is shifted down. Also, one can note that from Fig.2d the revival period is increased, and it can distinguish other periods of revival in that case, that is in the case of off-resonance for this case of  $\theta$  the revival period is more apparent. In fact the revival time is given by:  $\left(\tau_R = 2\pi G \sqrt{\delta^2 + |\alpha|^2}\right)$  which increases by increasing  $\delta$ . However, we can see from Fig.2d, that the detuning parameter leads to the state of qubit to tend to  $|g\rangle$  more than  $|e\rangle$ . Besides that, if  $\frac{\gamma}{G} \neq 0$ , the collapses and revivals phenomenon is still observed in a very short time. This phenomenon disappears slowly by increasing time due to the influence of  $\frac{\gamma}{G}$ . One can observe rapid deterioration for the revivals of  $W_{qu}$  at the large values of  $\frac{\gamma}{G}$ . From Fig.2d, we observe increasing in the behavior of  $W_{qu}$  curve, after that the value of  $W_{qu}$  is almost to zero at time  $Gt \simeq 50\pi$ . Moreover, the collapse region has becomes very large. However, if we take large values of  $\frac{\delta}{G}$  for the different values of  $\theta$ , the amplitudes of the fluctuations are diminished, the collapse periods are elongated, and a large decrease is happened in the amplitudes of periodic oscillations of maximum value and minimum value for the inversion.

## 3.2 Dynamical properties of coherence and entanglement phenomena

In order to understand the influence of dispersive reservoir of qubit on some dynamical properties, such as coherence and entanglement, we use in the following the solution in Eq.9. Then we investigate the effect of dispersive reservoir on the dynamical properties.

### 3.2.1 Dynamical properties of coherence phenomenon

In this part, we study the behavior of purity as a measure of the amount of coherence loss caused by the dispersive reservoir of qubit and the unitary qubit-vibrational mode interaction. The purity of this state is measured by the von Neumann entropy [32] as follows:

$$S_{qu(r)}(t) = - \sum_{i=1}^{\infty} \lambda_{qu(r)}^i(t) \ln \lambda_{qu(r)}^i(t), \quad (11)$$

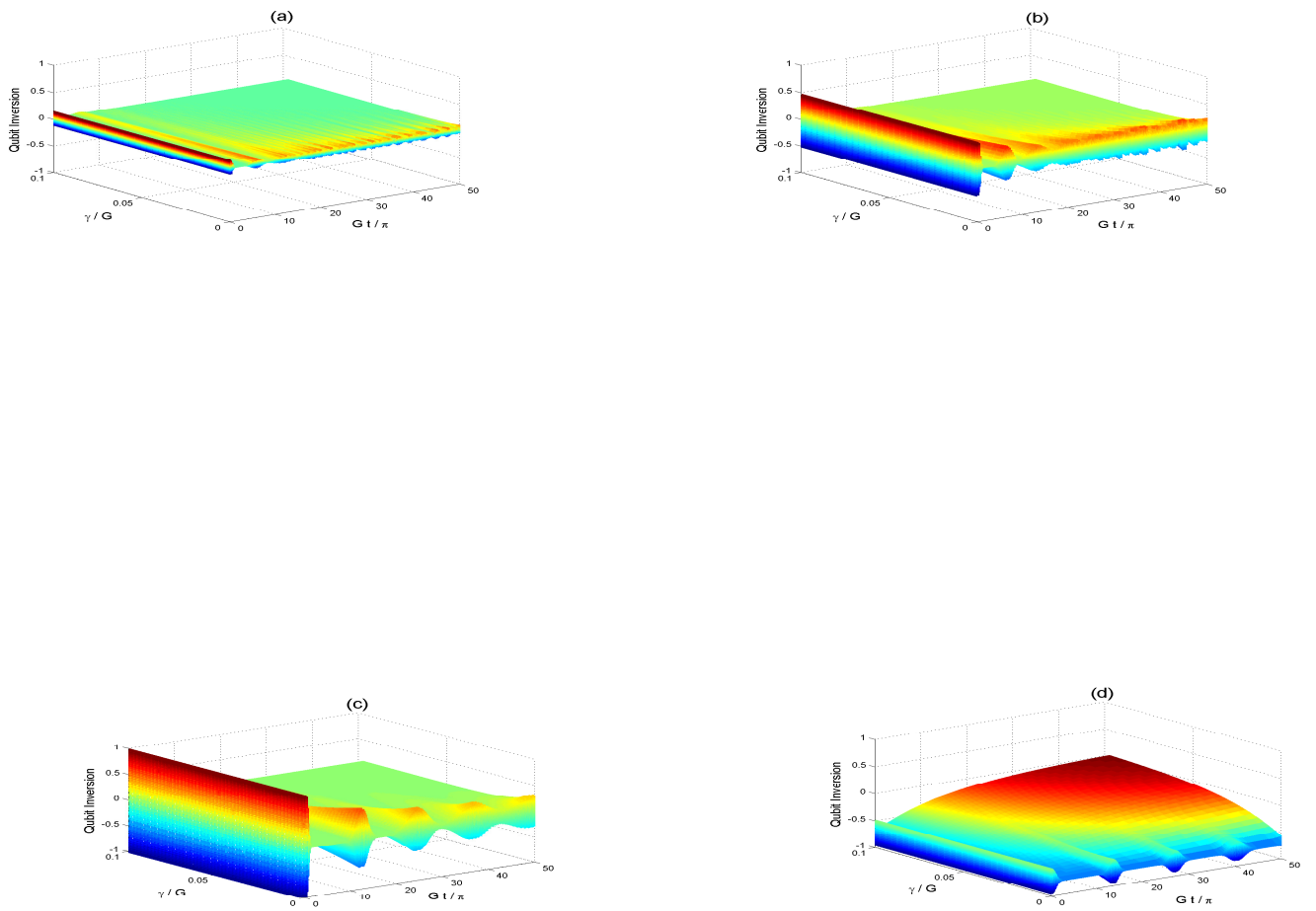


Figure 2: The evolution of SC qubit inversion plotted against the scaled time  $\frac{Gt}{\pi}$  and dispersive reservoir  $\frac{\gamma}{G}$  in the resonance case for  $\theta = \frac{\pi}{10}$  in (a),  $\theta = \frac{\pi}{3}$  in (b) and  $\theta = \frac{\pi}{2}$  in (c), and off-resonance case for  $\theta = \frac{\pi}{3}$  and  $\frac{\delta}{G} = 6$  in (d), with the coherence parameter  $\alpha = 3$  in (a, b, d) and  $\alpha = 6$  in (c).



where  $\lambda_{qu(r)}^i$  are the instantaneous eigenvalues of the two subsystems (qubit and torsional resonator). In a bipartite quantum system, the system and subsystem entropies, at any time  $t$ , are limited by the following Araki-Lieb inequality  $|S_{qu} - S_r| < S < |S_{qu} + S_r|$ . As a result, if the density operator  $\rho$  describes a pure state, the entropy  $S$  becomes 0 and remains constant. This means that, if the system is initially prepared in a pure state at any time  $t > 0$ , the reduced entropies of the two subsystems are identical, that is,  $S_{qu}(t) = S_r(t)$ . Otherwise  $S > 0$ , that is,  $S_{qu}(t) \neq S_r(t)$ .

Here, we begin from pure state, therefore, we either use  $S_r$  or  $S_{qu}$  in the absence of dispersive reservoir, to measure the amount of entanglement between the two subsystems, whether in the resonance or off-resonance cases. Exactly,  $S_{qu}(0) = S_r(0) = 0$ . In this work, we devote our study to the von Neumann entropy for the reduced density operator of the qubit that can be expressed as follows:

$$S_{qu}(t) = - \sum_{i=\pm} \lambda_{qu}^i(t) \ln \lambda_{qu}^i(t), \quad (12)$$

where  $\lambda_{qu}^{\pm}(t) = \frac{1}{2} \left( \rho_{ee}^{00} + \sum_{n=0}^{\infty} [\rho_{ee}^{n,n}(t) + \rho_{gg}^{n,n}(t)] \right) \pm \sqrt{\Lambda_n^2(t) + \Upsilon_n^2(t)}$ , with  $\Lambda_n(t) = \frac{1}{2} \left( \rho_{ee}^{00} + \sum_{n=0}^{\infty} [\rho_{ee}^{n,n}(t) - \rho_{gg}^{n,n}(t)] \right)$  and  $\Upsilon_n(t) = \left| \sum_{n=0}^{\infty} \rho_{ge}^{n,n+1}(t) \right|$ . In our discussion for the influence of dispersive reservoir of qubit on the purity, the time evolution of the purity against  $\frac{Gt}{\pi}$  and  $\frac{\gamma}{G}$ , in the resonance case with  $\theta = \frac{\pi}{3}$ ,  $\varphi = 0$  and  $\alpha = 3$ , is displayed in Fig.3a. From Fig.3a, if  $\frac{\gamma}{G} = 0$ , one can observe that the behavior of curve of  $S_{qu}$  is not periodical. In addition, we see that the time evolution curve of qubit entropy has local extreme at the revival time  $\left( t_R = \frac{2\pi|\alpha|}{G} = 3\sqrt{8I_m\omega/E_J\omega_z f'^2} \right)$ , indicating that the qubit state does not return most closely to its initial state at this time. Also, one can observe that the value of minima for  $S_{qu}$  in Fig.3a is increased when the time increases. Finally, the  $S_{qu}$  oscillate around its maxima as time becomes very large. Besides that, in the presence of the dispersive reservoir  $\frac{\gamma}{G} \neq 0$ , we cannot use the  $S_{qu}$  as a measure for entanglement but we use it as a measure to the amount of the coherence loss of the qubit state. At a weak dispersive reservoir, one can find the amplitudes of the oscillations of entropy diminish rapidly, and the local extreme of the purity at half-revival time for the mentioned measure are still apparent, where at this time the qubit and vibration mode are approximately disentangled. If  $\frac{\gamma}{G} = 0.1$ , the amplitudes of the local extreme of the purity oscillations are more rapidly deteriorated. Due to damping, the amplitude of the purity of qubit is suppressed. Therefore, the qubit coherence loss may occur due to dephasing interactions of qubit with the vibration mode. However, the purity loses its coherence more than its gain due to dispersive reservoir, and finally completely loses coherence and fall into a statistically mixed state.

As well as, we investigate in Fig.3b and Fig.3c, 3d), the evolution of purity in off-resonance case with  $\varphi = 0$  and  $\alpha = 3$  for a different values of  $\theta$  and  $\frac{\delta}{G}$ . In the absence of  $\frac{\gamma}{G}$ , see Fig.3b, Fig.3c and Fig.3d, one can note that the detuning parameter affects the fluctuations in the temporal evolution for  $S_{qu}$ , and results in deterioration of the oscillations. One can also note from these figures, the local extreme for the mentioned measure are pronounced and still apparent in all curves. However, we see that the amplitudes of oscillations of purity are decreasing due to the increase of the value for  $\frac{\delta}{G}$  in these different figures, that is the detuning parameter improves the influence of dispersive reservoir on this phenomenon. In addition, when  $\frac{\gamma}{G} \neq 0$ , one can find from Fig.3b, Fig.3c and Fig.3d at a weak value of  $\frac{\gamma}{G}$ , that the local extreme for the mentioned measure is about to disappear. Also, one can observe at the high values of  $\frac{\gamma}{G}$ , that the amplitudes of oscillations for all curves are deteriorated completely, and the purity is increased monotonically and no longer equal zero due to the influence of the dispersive reservoir.

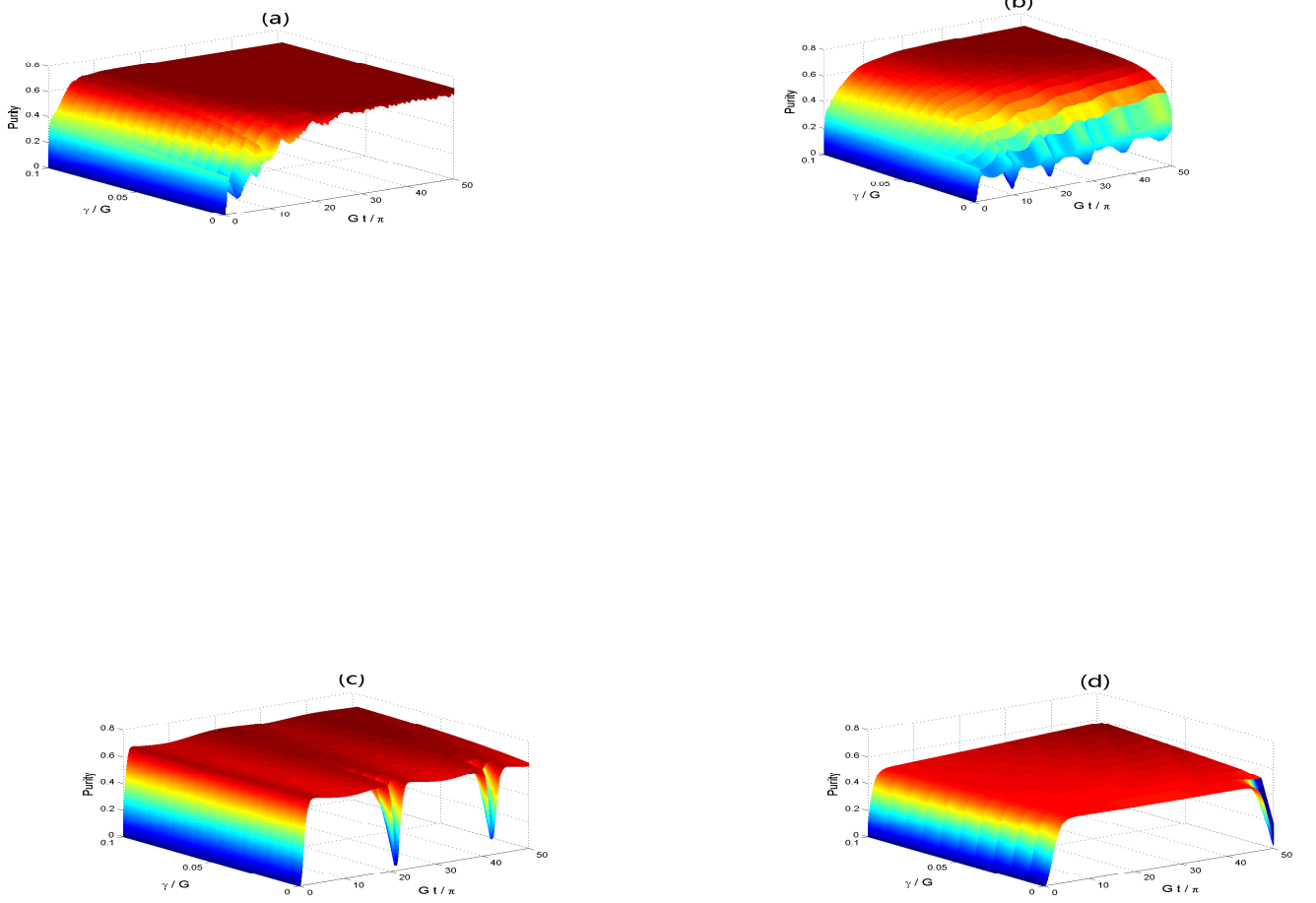


Figure 3: The evolution of purity plotted against the scaled time  $\frac{Gt}{\pi}$  and dispersive reservoir  $\frac{\gamma}{G}$  in the resonance case for  $\theta = \frac{\pi}{3}$  in (a), and off-resonance case for  $\theta = \frac{\pi}{3}$  and  $\frac{\delta}{G} = 4$  in (b),  $\theta = \frac{\pi}{4}$  and  $\frac{\delta}{G} = 10$  in (c) and  $\theta = \frac{\pi}{8}$  and  $\frac{\delta}{G} = 25$  in (d), with  $\alpha = 3$ .

However, from Fig.3c for  $\theta = \frac{\pi}{4}$  (phenomenon of coherent trapping) and  $\frac{\delta}{G} = 10$ , and from Fig.3d for  $\theta = \frac{\pi}{8}$  and  $\frac{\delta}{G} = 25$ . We note that the behavior for two curves of the purity in these cases of detuning is periodical, and note that the oscillations periods for two curves are apparent after a large period of time on the case in which  $\frac{\delta}{G} = 4$ . Then, we conclude that the behavior of curves of purity is also periodical for the values more than  $\frac{\delta}{G} = 25$  for the different values of  $\theta$ . Finally, when  $\frac{\gamma}{G} = 1$ , we get  $\lambda_{qu}^{\pm}(Gt \rightarrow \infty) = \frac{1}{2} \pm \frac{1}{2}e^{-|\alpha|^2} \cos^2 \theta$ , then  $S_{qu}(Gt \rightarrow \infty) \sim \ln 2 = 0.693$ , which means that the asymptotic qubit state is a statistically mixed state, that is the mixedness of the phase qubit state is complete.

### 3.2.2 Dynamical properties of entanglement phenomenon

Because of the existence of dispersive reservoir parameter in Eq.9, the purity cannot be a measure for the entanglement. Therefore, we use the negativity  $N(\rho)$  to measure the amount of the entanglement that can be expressed as [33]

$$N(\rho) = \max \left( 0, -\sum_s \lambda_s \right), \quad (13)$$

where  $\lambda_s$  is a negative eigenvalue of the partially transposed density matrix of the vibrational mode-phase qubit. Here,  $\lambda_s$  is computed by using numerical calculations. For an entangled mixed state,  $N(\rho)$  is positive. If  $N(\rho) = 0$ , the states are separable. Moreover, the negativity is used to estimate the amount of entanglement of the final state if we start with a pure or mixed state.

The influence of dispersive reservoir of qubit on the negativity as a function of  $\frac{Gt}{\pi}$  and a parameter  $\frac{\theta}{\pi}$  in the resonance case when  $\varphi = \frac{\pi}{4}$  and  $\alpha = 3$  is shown in Fig.4a and Fig.4b. From Fig.4a, in the absence of  $\frac{\gamma}{G}$ , we note that the local extremes of  $N(\rho)$  approximately are regularly distributed at small times  $Gt \simeq 10\pi$  with the different values of  $\theta$ . After that, the values of minimum for  $N(\rho)$  are increased when the time increases. Also, the time evolution curve of  $N(\rho)$  has a local extreme at the revival time  $t_R$ . However, we note that, the value of  $N(\rho)$  is oscillated around its maxima for the different values of  $\theta$  and  $Gt$ . If we take into account the dispersive reservoir parameter, the amplitudes of the fast oscillations of the negativity measure diminish, and  $N(\rho)$  arrives to its minima (maxima) value at half-revival time. The negativity has a very strong sensitivity to  $\frac{\gamma}{G}$  parameter. Therefore, when we take  $\frac{\gamma}{G} = 0.1$ , see Fig.4b, the  $N(\rho)$  quite vanishes at particular times for the different values of  $\theta$ . In this case, the dispersive reservoir at these particular times, the entanglement between the vibrational mode and qubit is completely destroyed. If  $N(\rho) = 0$ , the final state shown in Eq.9 disentangles completely and abruptly in just a finite time and evolves to the vacuum state, and its coherence is lost completely.

To visualize the influence of detuning parameter and  $\frac{\gamma}{G}$  parameter on the temporal evolution for negativity, the behavior of the negativity in off-resonance case with  $\theta = \frac{\pi}{7}$ ,  $\alpha = 3$  and  $\varphi = \frac{\pi}{4}$  is displayed in Fig.4c and Fig.4d. One can find that, the detuning parameter  $\frac{\delta}{G} \neq 0$  affects the amplitudes of fluctuations in the evolution of  $N(\rho)$  either by increasing or by decreasing on the case in which  $\frac{\delta}{G} = 0$  for the different values of  $\theta$ . Therefore, if  $\theta = \frac{\pi}{7}$ , see Fig.4c, the amplitudes of oscillations of  $N(\rho)$  are less than their counterparts of the case  $\frac{\delta}{G} = 0$ . Because of the detuning parameter, some of oscillations are deteriorated, the local extremes of the negativity are pronounced and still apparent in this surface. In addition, with  $\frac{\gamma}{G} \neq 0$ , the oscillations of the local extreme of the  $N(\rho)$  are disappeared completely. When the dispersive reservoir is increased, say  $\frac{\gamma}{G} = 0.1$ , see Fig.4d, the amplitude of most oscillations are suppressed and  $N(\rho)$  quite vanishes at particular times. This means that, after a particular time, the dispersive reservoir destroys the entanglement of the global total system state. Therefore, one

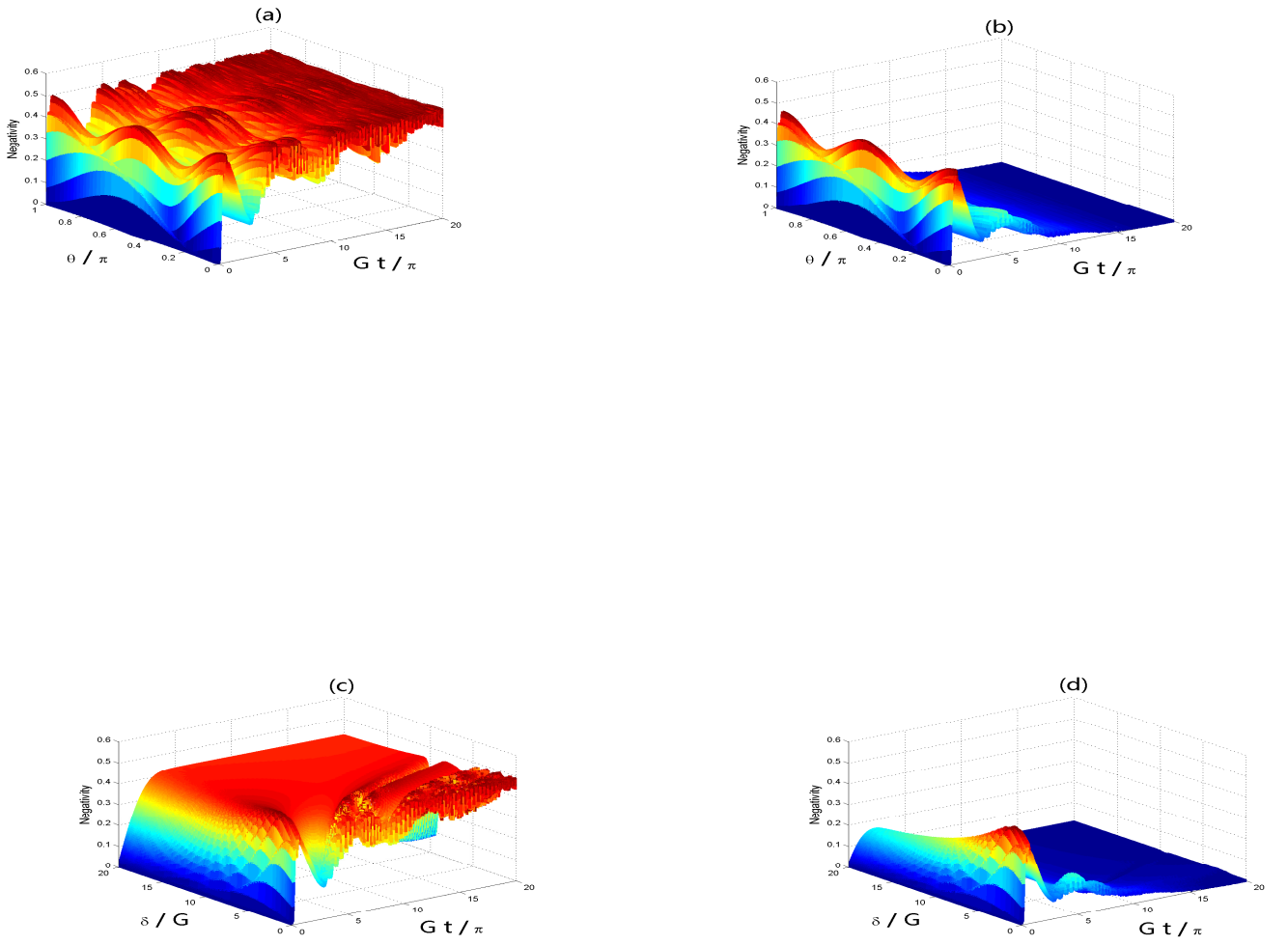


Figure 4: The time evolution of the entanglement  $N(\rho)$  in the resonance case for all  $\theta$  and off-resonance case for  $\theta = \frac{\pi}{7}$ , with  $\varphi = \frac{\pi}{4}$  and  $\alpha = 3$ , for the different values of dispersive reservoir:  $\frac{\gamma}{G} = 0$  in (a, c) and  $\frac{\gamma}{G} = 0.1$  in (b, d).

can determine a particular region in which there is no entanglement between the qubit and the torsional resonator due to the complete destruction of coherence in the presence of  $\frac{\gamma}{G}$ .

## 4 Conclusion

In this article, the system of SC phase qubit coupled to a torsional resonator is governed by a master equation. An analytical solution for the master equation is obtained with the general initial state. Several physical phenomena have been studied, such as qubit inversion, purity and negativity in the resonance and off-resonance cases for many different initial states. It is found that, the qubit inversion and purity, for the resonance and off-resonance cases, are quite sensitive to any change  $\frac{\gamma}{G}$  parameter. By using the negativity the amount of the entanglement is studied. The dispersive reservoir destroys the entanglement of the global vibrational mode-phase qubit state. In addition, we found that in off-resonance case, the detuning parameter improve the influence of the damping on qubit inversion, purity and negativity. Therefore, one can determine a particular region in which there is no entanglement between the qubit and the torsional resonator due to the presence of  $\frac{\gamma}{G}$ .

## References

- [1] C. H. Bennet, G. Brassard, C. Crepeau, R. Josza, A. Peres and W. K. Wothers, *Phys. Rev. Lett.* **70** (1993) 1895.
- [2] C. H. Bennet and S. J. Wiesner, *Phys. Rev. Lett.* **69** (1992) 2881.
- [3] J. A. Wheeler and Z. H. Zurek, Quantum Theory of Measurement, *Princeton University Press, NJ* (1983).
- [4] A.-S. F. Obada, H. A. Hessian and A.-B. A. Mohamed, *Opt. Commun.* **280** (2007) 230; *Phys. Lett. A* **372** (2008) 3699; *Commun. Theor. Phys.* **51** (2009) 723; *J. Mod. Optics.* **56** (2009) 881.
- [5] H. A. Hessian and H. Ritsch, *J. Phys. B*, **35** (2002) 4619.
- [6] A.-S. F. Obada and A.-B. A. Mohamed; *Opt. Commun.* **285** (2012) 3027; *Solid State Commun* **151**(2011) 1824; *Opt. Commun.* **309** (2013) 236.
- [7] A.-B. A. Mohamed, *Phys. Lett. A* **374** (2010) 4115; *Int. J Quant. Information* **9** (2011) 19; *Ann. Phys.* **327** (2012) 3130; *Quantum Inf. Process* **12** (2013)1141.
- [8] C. P. Sun, H. Zhan and X. F. Liu, *Phys. Rev. A* **58** (1998) 1810.
- [9] L. M. Kuang, Z. Y. Tong, Z. W. Oyang and H. S. Zeng, *Phys. Rev. A* **61** (2000) 013608.
- [10] A.-S. F. Obada, Hosny A. Hessian, *J. Opt. Soc. Am. B.* **21** (2004) 1535; A.-S. F. Obada, H. A. Hessian and A.-B. A. Mohamed, *Laser Physics* **18** (2008)1111.
- [11] S. Abdalla, A.-S. F. Obada, E. M. Khalil and A.-B. A. Mohamed, *Solid State Commu.* **184** (2014) 56.
- [12] T. Yu and J. H. Eberly, *Phys. Rev. Lett.* **93** (2004) 140404; T. Yu, *Phys. Lett. A* **361** (2007) 287.

- [13] M. Yönaç, T. Yu and J. H. Eberly, *J. Phys. B: At. Mol. Opt. Phys.* **39** (2006) S621.
- [14] A-B A. Mohamed, H. A. Hessian and A.-S. F. Obada, *Physica A* **390**, 519 (2011)
- [15] M. Abdel-Aty, H. Moya-Cessa, *Physics Letters A* **369** (2007) 372.
- [16] A.-B. A. Mohamed, A.-S. F. Obada, *Optics Commun.* **285** (2012) 3027.
- [17] T. Yu and J. H. Eberly, *Phys. Rev. Lett.* bf97 (2006) 140403.
- [18] M. P. Almeida, M. F. de, M. Hor-Meyll, A. Salles, S. P. Walborn, P. H. R. Souto and L. Davidovich, *Science* **316** (2007) 579.
- [19] J. Laurat, K. S. Choi, H. Deng, C. W. Chou and H. J. Kimble, *Phys. Rev. Lett.* **99** (2007) 180504.
- [20] I. Chiorescu, P. Bertet, K. Semba, Y. Nakamura, C. J. P. M. Harmans and J. E. Mooij, *Nature* **431** (2004) 159.
- [21] A. Blais, R.-S. Huang, A. Wallraff, S. Girvin and R. Schoelkopf, *Phys. Rev. A* **69** (2004) 062320.
- [22] A. Wallraff, D. I. Schuster, A. Blais, L. Frunzio, R.-S. Huang, J. Majer, S. Kumar, S. M. Girvin and R. J. Schoelkopf, *Nature* **431** (2004) 162.
- [23] A.-S. F. Obada, H. A. Hessian, A.-B. A. Mohamed and Ali H. Homid, *J. Phys. A: Math. Theor.* **45** (2012) 485305; *Ann. Phys.* **334** (2013) 47.
- [24] A.-S. F. Obada, H. A. Hessian, A.-B. A. Mohamed and Ali H. Homid, *J. Opt. Soc. Am.* **30** (2013) 1178; *Quantum Inf. Process.* **13** (2014) 475.
- [25] Y. Nakamura, Y. A. Pashkin and J. S. Tsai, *Nature* **398** (1999) 786.
- [26] I. Tornes and D. Stroud, *Phys. Rev. B* **77** (2008) 224513.
- [27] J. M. Martinis, S. Nam, J. Aumentado and C. Urbina, *Phys. Rev. Lett.* **89** (2002) 117901.
- [28] M.-J. Hwang, J.-H. Choi and M.-S. Choi, *J. Phys. Condens. Matter* **22** (2010) 355301.
- [29] R. R. Puri and G. S. Agarwal, *Phys. Rev. A* **35** (1987) 3433.
- [30] A.-S. F. Obada, H. A. Hessian and A.-B. A. Mohamed, *J. Phys. B: At. Mol. Opt. Phys.* **40** (2007) 2241; *chin. phys. Lett.* **25** (2008) 949.
- [31] A.-S. F. Obada, H. A. Hessian and A.-B. A. Mohamed, *Ann. Phys.* **325** (2010) 519.
- [32] S. J. D. Phoenix and P. L. Knight, *Ann. Phys.* **186** (1988) 381.
- [33] A. Peres, *Phys. Rev. Lett.* **77** (1996) 1413.